LBL--29244

DE90 015720

VACUUM ARC ION CHARGE STATE DISTRIBUTIONS

Ian G. Brown and Xavier Godechot*

Accelerator and Fusion Research Division
Lawrence Berkeley Laboratory
University of California
Berkeley, CA 94720

Presented at the
14th International Symposium on
Discharges and Electrical Insulation in Vacuum,
Santa Fe, NM, September 16-20, 1990

* On leave to Lawrence Berkeley Laboratory from SODERN; present address SODERN, 1 Ave. Descartes, 94451 Limeil-Brevannes, France, Supported by a Grant from the French Ministère des Affaires Etrangère, Bourse Lavoisier, and a Grant from SODERN.

This work was supported by the U.S. Army Research Office under Contract No. ARO 116-89, the Office of Naval Research under Contract No. N00014-88-F-0093, and the Department of Energy under Contract No. DE-AC03-76SF00098.

VACUUM ARC ION CHARGE STATE DISTRIBUTIONS

Ian G. Brown and Xavier Godechot*

Lawrence Berkeley Laboratory
University of California
Berkeley, CA 94720

ABSTRACT

We have measured vacuum arc ion charge state spectra for a wide range of metallic cathode materials. The charge state distributions were measured using a time-of-flight diagnostic to monitor the energetic ion beam produced by a metal vapor vacuum arc ion source. We have obtained data for 48 metallic cathode elements: Li, C, Mg, Al, Si, Ca, Sc, Ti, V, Cr, Mn, Fe, Co, Ni, Cu, Zn, Ge, Sr, Y, Zr, Nb, Mo, Pd, Ag, Cd, In, Sn, Ba, La, Ce, Pr, Nd, Sm, Gd, Dy, Ho, Er, Yb, Hf, Ta, W, Ir, Pt, Au, Pb, Bi, Th and U. The arc was operated in a pulsed mode with pulse length 0.25 msec; arc current was 100 A throughout. This array of elements extends and completes previous work by us. In this paper the measured distributions are cataloged and compared with our earlier results and with those of other workers. We also make some observations about the performance of the various elements as suitable vacuum arc cathode materials.

I. INTRODUCTION

Charge state distributions of ions generated by the metal vapor vacuum arc have been reported previously by us [1-3] and also by several other workers [4-6]. In our work, we have used an ion source in which the metal vapor vacuum arc is used as the method of plasma production and from which high quality, high current beams of metal ions can be extracted [7-13]. We have called this source the MEVVA ion source, as an acronym for the plasma mechanism employed. Beams at voltages up to 100 kV and with ion currents up to 1 Ampere have been produced. The source works well with a wide range of ion species spanning the periodic table from lithium to uranium.

It is a goal of our experimental program to explore the utility of the MEVVA ion source for carrying out metallurgical surface modification by high dose metallic ion implantation. We have made a number of source embodiments; these sources are used on a test stand incorporating a time-of-flight (TOF) diagnostic for measurement of the charge state distribution (CSD) of the ion beam being used. Thus a survey of the charge state distributions of all the metal ion beams that we can produce can be readily accomplished.

Here we firstly give a brief description of the ion source and charge state diagnostic, and then present the results of our measurements. The results are compared with our prior work and also with the results of other workers, where such comparisons are available. The results presented here provide a large data base on vacuum arc ion charge state spectra.

II. EXPERIMENTAL SET-UP

For the measurements described here we have used the MEVVA V metal ion source. In this source 18 separate cathodes are mounted in a single cathode assembly, allowing the operational cathode to be changed simply by rotating an external knob. Thus many different cathode materials can be compared in a relatively short experimental run and with confidence in maintaining the same experimental conditions. The characteristics and performance of the MEVVA V are described in more detail in an accompanying paper [13].

In the MEVVA sources, an intense plume of highly ionized metal plasma that is created at the vacuum arc cathode spots provides the "plasma feedstock" from which the ion beam is extracted. The quasi-neutral plasma plumes away from the cathode toward the anode and persists for the duration of the arc current drive. The anode of the discharge is located on axis with respect to the cylindrical cathode and has a central hole through which a part of the plasma plume streams. The plasma drifts through the post-anode region to the set of grids that comprise the ion beam formation electrodes - a three grid, accel-decel, multi-aperture design.

The arc is driven by a simple pulse line. The line is a 6-section LC network of impedance 1 Ohm and pulse length 250 μs. The line is charged to a voltage of several hundred volts with a small, isolated, dc power supply. A high voltage pulse applied to a trigger electrode initiates a surface spark discharge between a trigger electrode and the cathode, which in turn causes the main anode-cathode circuit to close due to the spark plasma, and the vacuum arc proceeds. For all the measurements described here the arc current was 100 A. The source is typically operated at a repetition rate of from several up to about 20 or 30 pulses per second.

The source is operated on a test-stand equipped with various diagnostics to monitor the source performance and the parameters of the extracted beam. Base pressure is about 5×10^{-7} Torr range. For the measurements reported here the beam extraction voltage was 50 kV. Beam current was measured by a magnetically suppressed Faraday cup and was typically several hundred milliamperes.

The charge state distribution (CSD) of the extracted ion beam was measured using a time-of-flight (TOF) diagnostic [14]. In this method, a set of deflection plates is located in the beam path and biased so as to deflect the beam aside except for a short pulse of about 0.2 μs in length. This short beam pulse sample is drifted down a region of sufficient length to allow the different charge-to-mass (Q/A) components of the beam to separate out, since they have been accelerated through the same potential drop in the ion source extractor and thus have flight times proportional to $(Q/A)^{-1/2}$. A detector, a well-shielded Faraday cup with magnetic suppression of secondary electrons, at the end of the drift chamber, measures the arrival time of the different Q/A components of the beam. The beam is steered onto the detector by the annular gating plates, and the detector is prevented from viewing the intense visible light and UV generated by the vacuum arc by blocking the direct path with a metal plate which also serves as a beam current monitor. The detector measures the electrical current in the different charge states and provides a good measurement of the CSD of the extracted ion beam. The measured flight times for the various charge states are well fitted by the calculated values, usually to better than the measurement uncertainty of about 1%.

The cathodes were not prepared in any special way; the material used was regular stock material and the cathode surface was cleaned with alcohol. After a clean-up period of typically no more than a few hundred firings of the ion source the measured spectra were generally quite clean, with minimal impurity contamination visible. A schematic of the experimental configuration is shown in Figure 1.

III. RESULTS

A typical oscillogram of arc current and extracted ion beam current for the case of a titanium cathode is shown in Figure 2 (average of several shots). The beam current shown is that fraction of the beam detected by a 5 cm diameter Faraday cup at a distance of about 60 cm from the ion source extractor; the total extracted beam current is greater than this by a factor a several. Beam noise is typically about 5 to 10 %. Oscillograms showing typical TOF spectra are shown in Figure 3.

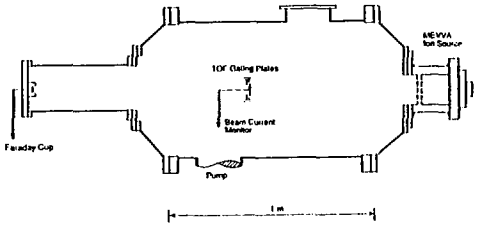

Fig. 1 Schematic of the experimental configuration. (XBL 896-7641)

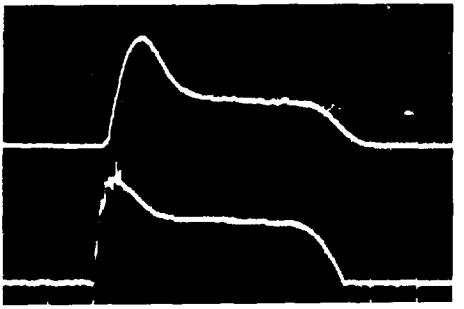

Fig. 2 Oscillogram showing typical ion beam and arc current traces for titanium.
Upper trace: ion beam current, 200 mA/cm;
Lower trace: arc current, 100 A/cm;
Sweep speed: 50 μs/cm. (XBB 904-2898)

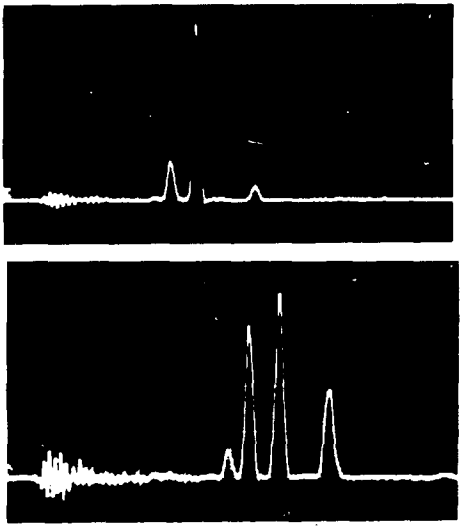

Fig. 3 Time-of-flight charge state spectra.
Upper: Ti; peaks are Q=1,2,3, right to left (XBB 904-2900)
Lower: Ta, peaks are Q=1,2,3,4,5, right to left (XBB 904-2899)

All data were taken for the same arc current, I_{arc} = 100 A, and for a beam extraction voltage V_{ext} = 50 kV. All the TOF spectral data were taken at a time of 150 μs after the beginning of the arc current pulse. Note that these spectra were obtained as ion current collected by a Faraday cup, and the amplitudes of the charge state peaks measured are thus in units of electrical current; the electrical current I_{elec} is greater than particle current I_{part} by the charge state Q,

$$I_{elec} = QI_{part} \qquad (1)$$

It can be important to distinguish between charge state distributions that are given in terms of electrical current fractions or particle current fractions.

The charge state distribution has been measured as a function of time throughout the arc current pulse for several different cathode materials. Experimentally this is readily accomplished by scanning the time-of-flight gating pulse through the arc pulse, since the TOF spectral measurement is essentially an instantaneous measurement (0.2 μs). An example of the results obtained is shown for the case of Ta in Figure 4. It can be seen that the distribution contains higher charge states at early times and decreases to a more or less steady state distribution after approximately 50 to 100 μs. Thus in terms of the steady-state charge state distributions we can dismiss the early *time behavior as an initial transient. The early-time behavior has* been described in more detail in ref [15].

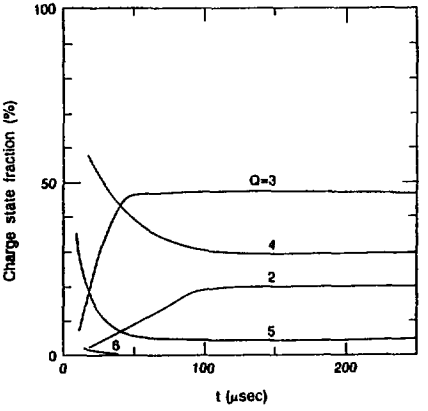

Fig. 4 Time history of the charge state spectrum (normalized particle fractions) throughout the arc current pulse for Ta. (XBL 896-7179)

The results obtained for the 48 solid metals that we investigated - Li, C, Mg, Al, Si, Ca, Sc, Ti, V, Cr, Mn, Fe, Co, Ni, Cu, Zn, Ge, Sr, Y, Zr, Nb, Mo, Pd, Ag, Cd, In, Sn, Ba, La, Ce, Pr, Nd, Sm, Gd, Dy, Ho, Er, Yb, Hf, Ta, W, Ir, Pt, Au, Pb, Bi, Th and U - are summarized is Table I. Here the charge state distributions are given in terms of normalized particle current fractions as determined from the TOF oscilloscope data using eqn (1). The mean charge state Q_p is then the mean with respect to the particle distribution.

We found that most metals trigger and form a discharge relatively easily using our standard trigger electrode and cathode configuration. Some metals, such as Ti and Mo, operate better than *others - they fire more easily (lower trigger voltage) and the arc* discharge produced is quiet and repeatable. Other metals, such as W and U, need a higher voltage trigger pulse and the arc is less stable. In general the arc discharge operates better (more repeatable and stable) at higher arc current.

TABLE I

Charge state fractions and mean charge states for the range of cathode materials studied here. Both the distributions and the means are expressed in terms of particle fractions. * Trace (under 1%)

ELEMENT	Z	Q=1+	2+	3+	4+	5+	6+	$\bar{Q}_p$
Li	3	100						1.0
C	6	100						1.0
Mg	12	46	54					1.5
Al	13	38	51	11				1.7
Si	14	63	35	2				1.4
Ca	20	8	91	1				1.9
Sc	21	27	67	6				1.8
Ti	22	11	75	14				2.1
V	23	8	71	20	1			2.1
Cr	24	10	68	21	1			2.1
Mn	25	49	50	1				1.5
Fe	26	25	68	7				1.8
Co	27	34	59	7				1.7
Ni	28	30	64	6				1.8
Cu	29	16	63	20	1			2.0
Zn	30	80	20					1.2
Ge	32	60	40	*				1.4
Sr	38	2	98					2.0
Y	39	5	62	33				2.3
Zr	40	1	47	45	7			2.6
Nb	41	1	24	51	22	2		3.0
Mo	42	2	21	49	25	3		3.1
Pd	46	23	67	9	1			1.9
Ag	47	13	61	25	1			2.1
Cd	48	68	32					1.3
In	49	66	34	*				1.4
Sn	50	47	53					1.5
Ba	56		100					2.0
La	57	1	76	23				2.2
Ce	58	3	83	14				2.1
Pr	59	3	28	69				2.7
Nd	60		83	17				2.2
Sm	62	2	83	15				2.1
Gd	64	2	76	22				2.2
Dy	66	2	66	32				2.3
Ho	67	2	66	32	*			2.3
Er	68	1	63	35	1			2.4
Yb	70	3	88	8				2.1
Hf	72	3	24	51	21	1		2.9
Ta	73	2	33	38	24	3		2.9
W	74	2	23	43	26	5	1	3.1
Ir	77	5	37	46	11	1		2.7
Pt	78	12	69	18	1			2.1
Au	79	14	75	11				2.0
Pb	82	36	64					1.6
Bi	83	83	17					1.2
Th	90		24	64	12			2.9
U	92		12	58	30			3.2

The use of semiconductors such as Si and Ge is more difficult because of their lower conductivity. There is a voltage drop and power dissipation in the cathode and the behavior of the arc is more erratic. The solution is to use a cathode fabricated from highly doped material, which is then more conductive. We have successfully done this for Si.

IV. DISCUSSION

We now compare the results obtained in the present work to our previous results [1,2] and to those of other workers [4-6]. Results have been presented in the literature of charge state distributions for a number of different cathode materials. Although the 48 different elements reported on here constitute a much wider data base than previously available, it is none-the-less interesting to compare the present results with those previously reported.

A comparison of charge state distribution data obtained here with such data as are available from a number of other sources is shown in Table II. In all cases the CSD is that of the ions generated by the cathode spots but measured at a distance from the cathode. Arc current was not greatly different between the various experiments, and in any case we have found that the CSD changes only minimally with arc current; the currents used in the different experiments are noted in the Table. The distributions have been expressed in terms of normalized particle fraction, the same as in Table I. The distinction between electrical current and particle current, which is very important for multiply charged ions and can make a big difference in the quoted distributions, seems to have not always been made clear in the literature. In particular, it is not clear to us if the references used for comparison have quoted electrical current or particle current. Depending on the detector used for measurement of the charge state spectrum, the signal can be J_{elec} or J_{part} or somewhere in-between; see reference 14 for an experimental investigation of this concern. In any case, the differences between our results and those of other workers, for those cases for which comparisons can be made, are not great. Our results cover most of the solid metals and greatly extend the data.

The new data compare fairly well with our previously reported results. For the most part the new data show slightly higher charge states than previously reported. We can speculate upon the origin of the differences, and further work would certainly help clarify the situation. But the differences are not great, and we take this as an indication of the inherent experimental uncertainty in our measurement technique.

We have looked at the measured mean charge state, $\bar{Q}_p$, as a function of atomic number Z and boiling point T_{BP} of the cathode material. In Figure 5 the particle mean charge state is shown as a function of atomic number. There is a trend in the data when so plotted but the fit is best when plotted against the boiling point temperature. In Figure 6 the mean charge state $\bar{Q}_p$ is plotted as a function of boiling point (°C) for all the elemental cathode materials investigated here. The straight line shown has been obtained through a linear regression (least squares best fit) to the data points, excluding carbon which show the greatest departure from the trend. The line is given by

$$\bar{Q}_p = 0.38(T_{BP}/1000) + 1 \qquad (2)$$

This expression provides a reasonably good fit to the data, apart from carbon, with a correlation coefficient of 0.68, and could be used as an empirical predictor.

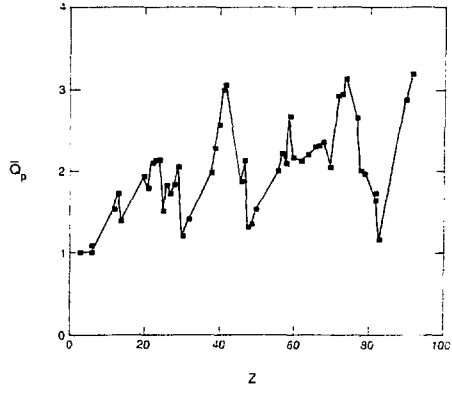

Fig. 5 Measured mean charge state, $\bar{Q}_p$, as a function of atomic number Z. (XBL 906-6415)

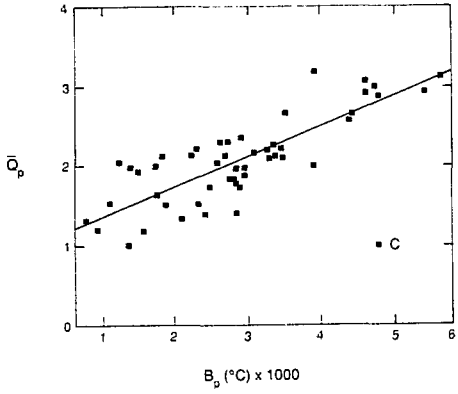

Fig. 6 Measured mean charge state, $\bar{Q}_p$, as a function of boiling point temperature T_{BP} (°C) of the cathode material. The straight line is the best fit to the data points (except carbon) and is given by $\bar{Q}_p = 0.38(T_{BP}/1000) + 1$. (XBL 906-6416)

V. CONCLUSION

Measurements have been made of the charge state distribution of the ions produced by the metal vapor vacuum arc for most of the solid metals of the Periodic Table. In general multiply charged ions are produced and the mean charge state, $\bar{Q}_p$, increases with the boiling point of the cathode material. An approximate phenomenological fit to the data is provided by the formula $\bar{Q}_p = 0.38(T_{BP}/1000) + 1$, where $\bar{Q}_p$ is the mean charge state in terms of particle current and T_{BP} is the boiling point temperature in °C. The charge state distribution measurements presented here are generally consistent with our previous work and the results of other workers.

ACKNOWLEDGMENTS

We are greatly indebted to Bob MacGill and Mike Dickinson for the mechanical design and fabrication of the ion source and other experimental facilities, and to Jim Galvin for the electronics and electrical design and support, and for their continued invaluable contributions throughout the experimental program. This work was supported by the U.S. Army Research Office and the Office of Naval Research under Contract No. ARO 116-89 and by the Department of Energy under Contract No. DE-AC03-76SF00098.

* On leave to Lawrence Berkeley Laboratory from SODERN; present address SODERN, 1 Ave. Descartes, 94451 Limeil-Brevannes, France. Supported by a grant from the French Ministère des Affaires Etrangères, Bourse Lavoisier, and a grant from SODERN.

TABLE II

Comparison of the charge state distributions (particle fractions) measured in the present work with those obtained by us previously and with the results of other authors. This work, arc current = 100 A, accelerating voltage 50 kV; Ref. 1,2, arc current 200 A, accelerating voltage 60 kV; Ref. 4 arc current mostly 100 A; Ref. 5, 100 A except Ta 140 A; Ref. 6, 100 A except Mo 170 A. * Trace (under 1%)

Element	Author	Charge State Fraction (%) Q=1+	2+	3+	4+	5+	6+	$\bar{Q}_p$
C	This work	100						1.0
	Ref 1,2	100						1.0
	Ref 5	96	4					
Mg	This work	46	54					1.5
	Ref 1,2	37	63					1.6
	Ref 4	50	50					
Al	This work	38	51	11				1.7
	Ref 1,2	56	39	5				1.5
	Ref 4	60	38	2				
	Ref 5	49	44	7				
Si	This work	63	35	2				1.4
	Ref 1,2	56	42	2				1.5
Ca	This work	8	91	1				1.9
	Ref 5	53	47	*				
Ti	This work	11	75	14				2.1
	Ref 1,2	6	82	12				2.1
	Ref 6	27	67	6				
Cr	This work	10	68	21	1			2.1
	Ref 1,2	25	67	8				1.8
	Ref 6	16	68	14	2			
Fe	This work	25	68	7				1.8
	Ref 1,2	31	64	5				1.7
	Ref 6	54	46		0.5			
Co	This work	34	59	7				1.7
	Ref 1,2	47	49	4				1.6
Ni	This work	30	64	6				1.8
	Ref 1,2	53	44	3				1.5
	Ref 4	65	33	2				
	Ref 5	48	48	3	*			
Cu	This work	16	63	20	1			2.0
	Ref 1,2	44	42	14				1.7
	Ref 5	30	54	15	0.4	*		
	Ref 6	38	55	7	0.5			
Zn	This work	80	20					1.2
	Ref 1,2	86	14					1.1
Zr	This work	1	47	45	7			2.6
	Ref 1,2	9	55	30	6			2.3
	Ref 5	14	60	21	5	*		

Element	Author	Charge State Fraction (%) Q=1+	2+	3+	4+	5+	6+	$\bar{Q}_p$
Nb	This work	1	24	51	22	2		3.0
	Ref 1,2	5	46	37	12			2.6
Mo	This work	2	21	49	25	3		3.1
	Ref 1,2	14	47	28	11			2.4
	Ref 5	16	69	13	1.5			
	Ref 6	3	33	42	19	3		
Pd	This work	23	67	9	1			1.9
	Ref 1,2	39	57	4				1.6
Ag	This work	13	61	25	1			2.1
	Ref 1,2	32	59	9				1.8
	Ref 5	65	34	1				
Cd	This work	68	32					1.3
	Ref 4	99.7	0.3					
In	This work	66	34	*				1.4
	Ref 1,2	88	12					1.1
Sn	This work	47	53					1.5
	Ref 1,2	53	47					1.5
Gd	This work	2	76	22				2.2
	Ref 1,2	6	81	13				2.1
Ho	This work	2	66	32				2.3
	Ref 1,2	15	76	9				1.9
Ta	This work	2	33	38	24	3		2.9
	Ref 1,2	13	39	28	18	2		2.6
	Ref 5	13	35	28	13	10	0.3	
W	This work	2	23	43	26	5	1	3.1
	Ref 1,2	8	34	36	19	3		2.7
Pt	This work	12	69	18	1			2.1
	Ref 1,2	69	29	2				1.3
Au	This work	14	75	11				2.0
	Ref 1,2	44	54	2				1.6
Pb	This work	36	64					1.6
	Ref 1,2	64	36					1.4
Th	This work		24	64	12			2.9
	Ref 1,2	3	15	70	12			2.9
U	This work		12	58	30			3.2
	Ref 1,2	3	38	54	5			2.6

REFERENCES

1. I. G. Brown and J. E. Galvin, XIIIth ISDEIV, Paris, 1988, p. 214. Also published in IEEE Tran. Plasma Sci. PS-17, 679 (1989).
2. I.G.Brown, B.Feinberg and J.E. Galvin, J. Appl. Phys. 63, 4889 (1988).
3. J. Sasaki and I. G. Brown, J. Appl. Phys. 66, 5198 (1989).
4. A. A. Plyutto, V. N. Ryzhkov and A. T. Kapin, Sov. Phys. JETP 20, 328 (1965).
5. W. D. Davis and H. C. Miller, J. Appl. Phys. 40, 2212 (1969).
6. V. M. Lunev, V. G. Padalka and V. M. Khoroshikh, Sov. Phys. Tech. Phys. 22(7), 858 (1977).
7. I. G. Brown, J. E. Galvin and R. A. MacGill, Appl. Phys. Lett. 47, 358 (1985).
8. I. G. Brown, J. E. Galvin, B. F. Gavin and R. A.MacGill, Rev. Sci. Instrum. 57, 1069 (1986).
9. I. G. Brown, in "The Physics and Technology of Ion Sources", edited by I. G. Brown, p. 331, (Wiley, N.Y., 1989).
10. R. A. MacGill, I. G. Brown and J. E. Galvin, Rev. Sci. Instrum. 61, 580 (1990).
11. I. G. Brown, J. E. Galvin, R. A. MacGill and F. J. Paoloni, Rev. Sci. Instrum. 61, 576 (1990).
12. H. Shiraishi, I. G. Brown, Rev. Sci. Instrum. 61, 589 (1990).
13. I. G. Brown, M. R. Dickinson, J. E. Galvin, X. Godechot and R. A. MacGill, "Metal Vapor Vacuum Arc Ion Sources", paper presented at this conference.
14. I. G. Brown, J. E. Galvin, R. A. MacGill and R. T. Wright, Rev. Sci. Instrum. 58, 1589 (1987).
15. J. E. Galvin, I. G. Brown and R. A. MacGill, Rev. Sci. Instrum. 61, 583 (1990).